Calibrated displacement prediction accuracy using the substitute structure method

NZSEE 2002
Conference

M.R. Edwards, J.L. Wilson, & N.T.K. Lam

Department of Civil and Environmental Engineering, The University of Melbourne

ABSTRACT: Considerable research has been undertaken in assessing the displacement response of structural systems to earthquake ground motion. As part of performance based seismic design, methods have been presented in several structural assessment documents enabling practitioners to make some prediction of peak displacement. This paper describes some of the research that has been undertaken to examine the nature of deformation and damping in reinforced concrete frame systems with a particular focus on the substitute structure method. The findings have been incorporated into a detailed time history analysis model that has, in turn, been used to calibrate a linear idealisation of response. Comparisons made with other published predictive methods have been encouraging for the limited structure range considered. The results suggest that a substitute structure methodology can be calibrated to provide an improved prediction of maximum displacement response when compared with other published methods.

1 INTRODUCTION

In recent years there has been much research interest in displacement based seismic evaluation and design of structures. This interest has, in part, been prompted by observations made of the performance of structures in large earthquakes. Survivability is observed to be more influenced by displacement capability than strength. Further, at serviceability response levels, non-structural damage to architectural components is largely related to drift. Consequently, for reliable performance based seismic design, accurate assessment of displacements at several limit states is required.

To assist in assessing the structural adequacy of existing buildings, both ATC-40 and FEMA 273 provide methodologies for predicting maximum displacement response to a given seismicity level. These predictions can be compared to an assessment of the structural systems displacement capability and conclusions drawn. Other researchers (Priestley et al 2000) have proposed methods that make the displacement assessment the basis for the design process itself.

Research work has been undertaken at the University of Melbourne to refine the existing ATC-40 predictive method which utilizes the Capacity Spectrum approach described by Freeman (Freeman 1998). The work seeks to complement well developed seismicity work already undertaken at the University (Lam et al 2002) by developing tools to both quantify displacement demand and to assess deformation capacity. Reinforced concrete special moment resisting frame (SMRF) systems dominated by first modal response have been considered, with results presented herein for a single degree of freedom (SDOF) type frame.

2 PREDICTIVE METHODS

The basis of most current code methods for displacement prediction is the equal displacement observation of Newmark and Hall. While a useful observation, scatter in the predictions is great, with significant errors associated with shorter period structures in the equal energy regime. Further research has served to improve the average predictions made, and a refined equal displacement based method forms the basis of the Coefficient Method of FEMA 273. Despite these refinements, the approach continues to predict inelastic displacements from the nominally elastic period part of the spectrum.

ATC-40 uses the Capacity Spectrum approach proposed by Freeman in an alternative approach. The structural period of a substitute linear system is progressively adjusted with the damping and damped elastic spectra updated. Convergence is achieved when the updated spectra and an adaptation of the structures push-over curve intersect at the adjusted period. This method focuses on the portion of the spectra associated with inelastic response, but requires a calibrated damping model to optimise displacement predictions.

One further approach is to use inelastic spectra, as described by Chopra (Chopra et al 1999). The hysteretically damped response of real structures is automatically incorporated into the spectra, for a structure having the same SDOF hysteretic characteristics as that used to generate the spectra, the displacement prediction is exact. Uncertainties are associated with the computational need to simplify and generalise real structural behaviour to generate the inelastic spectra.

3 INELASTIC MODELLING OF STRUCTURAL RESPONSE

To calibrate any predictive method, the inelastic response due to a given ground motion needs to be accurately determined by time history analysis (THA). The conventional approach is to model pre-yield damping viscously, with additional post-yield damping introduced hysteretically. In this research a refined THA has been adopted in which pre-yield softening and damping have been incorporated using hysteretic components.

Ductility can be defined in three basic ways; curvature ductility, rotational ductility, and global displacement ductility. Curvature ductility is mainly associated with adequate sub-assemblage performance, whereas rotational ductility reflects the aggregated contributions of the plastic hinge region to inelastic hinge rotation. In this research rotational ductility has been utilised as a measure of the inelastic demand on a component hinge. Connection between rotational ductility and global ductility can subsequently be made using the deformation model described below.

For rotational ductility, the hinge region has been assumed to consist of the beam/column joint and the portion of the member extending 1.8 times its depth from the face of the transverse framing member. Deformations consisted of the aggregate of joint shear distortion, strain penetration, and hinge flexural curvature. Shear deformations were treated separately. The point of "yield" was defined at first tensile yield, or when the extreme concrete compression strain reaching 0.2%, whichever was encountered first.

Global ductility was determined from the pushover curve of the generalised SDOF system. The portion of the curve up the ultimate load was generalised to a bi-linear approximation, with the area under the bi-linear curve matched to that under the real pushover curve. Post ultimate maximum displacement capacity was defined as that associated with a 20% loss of strength over 4 cycles, or 50 % strength loss in any hinge in the frame system.

4 SUBASSEMBLAGE DEFORMATION MODEL

A deformation model is required for the individual sub-assemblages that make up the system to

relate hinge behaviour to frame response. The principal frame deformation components identified were modelled and calibrated against experimental data.

The curvature distribution of the framing member was evaluated using moment/curvature software and used to determine flexural rotations and deformations. The Bernoulli assumption of plane sections remaining plane was made, but corrections were applied for post-yield conditions.

Park and Paulay's (Park and Paulay 1975) model for shear distortions was used up to yield. The model's shear stiffness was locally reduced for post-yield behaviour where non-closing flexural/shear cracks form.

The bar development model proposed by Alsiwat (Alsiwat et al 1992) was adopted to evaluate rotation at the face of transverse framing members due to strain penetration into beam/column joints. Rotation was assumed to occur about a constant neutral axis depth. The clamping effects of column axial loads on beam column joints were addressed using bond accentuation relationships determined by Soroushian (Soroushian et al 1991).

The monotonic joint shear distortion was determined using a simplified model proposed by Bonacci (Pantazoupolou and Bonacci 1992) with corrections applied for post-yield cyclic behaviour. Experimental work suggested a dependency of post-yield joint shear stiffness on rotational ductility demand. Relationships were regressed from the data that modify Bonacci's monotonic joint shear stiffness as rotational ductility demand increases beyond unity.

Post-elastic cyclic response differs from monotonic, being very loading history dependent. The Bernoulli assumption is no longer valid as diagonal shear cracks form and link with flexural cracks. Including the added effect of cyclic degradation, the uncorrected deformation model as described above provides an upper bound envelope to the hysteresis loops. The difference between the monotonic and cyclic envelopes was addressed empirically rather than mechanistically. For member hinges the collective rotational distortions were modelled as a combined spring possessing piecewise linearities. Parameters were derived from experimental data to assign stiffnesses to this combined spring, both up to ultimate, and beyond to failure.

The predicted yield load deflections were calculated and compared to the experimental results to check the overall validity of the combined deflection model. In Figure 1 the results from 27 beam hinges of 24 specimens tested by 9 different researchers are compared. On average the match is satisfactory although some scatter is observed.

5 NATURE OF STRUCTURAL DAMPING

As part of the research, the structural damping in reinforced concrete SMRF was examined and quantified using the same set of experimental data used for the deformation model. Pre-yield damping was examined separately, and shear damping mechanisms for beams were uncoupled from the flexural. The area method for assigning an equivalent viscous damping (EVD) level was adopted. In making this selection, the need to adjust the reference values obtained to optimise displacement prediction accuracy was acknowledged and addressed. Key findings are discussed below.

5.1 *Pre-yield global damping*

Within the pre-yield range there are no discrete hinges formed. Energy absorption is distributed throughout the members, being more pronounced in regions of high moment. In examining sub-yield damping, the systems global behaviour was quantified. By focussing on the location for first yield, the damping obtained was related to the maximum moment normalised by that which would induce yield. The results obtained from seven sub-assemblage specimens tested at several amplitudes of pre-yield displacement are presented in Figure 2. The gradual increase of damping with moment amplitude is consistent with a system that is gradually becoming more

inelastic, and the value of 6.81% at yield compares favourably with published values in the literature.

5.2 *Post-yield shear damping*

Shear damping was investigated separately for beam hinges, as non-closure of flexural cracks can result in significant shear mechanism development. Low aspect ratio beams particularly exhibit lower overall damping due to a larger portion of the systems deflection being associated with shear, and due to high shear stresses that are associated with lower levels of shear damping.

It has been possible to evaluate the shear mechanism independently using test specimen data where the hinge zone has been continuously monitored for shear distortion. Shear damping at a rotational ductility of 1.0 was assumed equal to the system sub-yield damping at yield.

5.3 *Post yield flexural damping*

Beyond yield, damping is concentrated in plastic hinge regions. The more extensive the hinging in the frame system the greater the ductility and damping. Mander's idealisation of an elastic framing member was used to determine the flexural and shear strain energy of the framing members outside of the hinge region. The shear strain energy and shear energy absorption within the hinge region was also determined. By deducting these values from those for the entire sub-assemblage, the strain energy and damping associated with the flexural damping mechanism was calculated. For column hinges the shear and flexural damping mechanisms were left combined. The results obtained for SMRF type beam hinges are presented in Figure 3. Damping was found to increase sharply following flexural yield and the total data was grouped based on typical rotational ductility step size.

6 **GLOBAL RESPONSE MATCH**

A single degree of freedom reinforced concrete frame was designed and a RUAUMOKO model of the frame generated for damping calibration purposes. The deformation and damping models already described were utilised to obtain a frame that would as closely as possible resemble the behaviour of the real frame, were it constructed and tested. This work is described below.

6.1 *Sub-assemblage match*

The deformation and damping behaviour of each column and each beam sub-assemblage from transverse member face to point of inflection was matched to model the overall response of the frame system. This was achieved using a single component Giberson type member with multiple end springs. The arrangement for a beam member is illustrated in Figure 4.

Three rotational stiffness degrading bi-linear springs were used to match inelasticity and damping in the pre-yield regime. These progressively yielded with increasing response from 20% of the yield moment upwards. Shear deformation and damping in the hinge zone was modelled separately using a single transverse spring having Sina type hysteresis. Finally, for additional post-yield flexibility and damping, two rotational Modified Takeda strength degrading springs were used that permitted a separate definition of both the negative and positive cyclic envelopes. Spreadsheets were developed to evaluate the associated 40 RUAUMOKO parameters.

6.2 *Single storey structural design*

The two storey reinforced concrete building used for calibration had a single level of seismic response due to a steel framed upper floor. It was designed using IBC 2000 and ACI-318 for Californian seismicity. A one-way pre-cast floor system resulted in seismic loading dominance for the ductile frames. Fixed base columns were assumed with no foundation compliance affecting displacement capability nor damping. The ductile mechanism was side-sway with

column hinging at both top and bottom.

6.3 *Single storey THA model*

Each sub-assemblage was matched as per Section 6.1 using damping values associated with large rotational ductility step sizes. Having matched the sub-elements, these were assembled into a non-linear model for analysis using RUAUMOKO. The final model was comprised of some 74 inelastic springs.

Sub-yield damping was assigned two ways. The cyclic push-over model used to obtain the global damped behaviour was modelled with all sub-yield damping incorporated hysteretically. The model used for earthquake THA work had the target sub-yield hysteretic damping reduced by 1% across the full range, with 1% Rayleigh type damping substituted.

6.4 *Single storey global response*

The global yield displacement was determined from a monotonic pushover analysis to be 38.7mm (1% drift approx). The frame was then subjected to a cyclic pushover both in the pre-yield and at post-yield ductility steps of 0.5. The area method based damping values obtained can be seen in Figure 5.

7 **CALIBRATION**

The reference damping curve presented in Figure 5 was adjusted to optimise prediction accuracy using the RUAUMOKO model developed and a suite of filtered earthquake records.

7.1 *Methodology*

The calibration procedure was as follows:-

1. Subject the model to a sequentially amplified record of each earthquake ground motion to induce progressively increasing displacement response.
2. Determine the maximum displacement response and the secant period at that point.
3. From a family of DRS for the ground motion, determine by scaling and interpolation which equivalent viscous damping level for the equivalent linear system would have matched the displacement. This is illustrated in Figure 6.
4. Determine the damping correction factor “Lambda” that would adjust the area method value at that ductility level to the value that would match the displacement
5. Regress the collective “Lambda” value set for all ground motions to optimise displacement prediction accuracy for the system at all amplitudes of response.

7.2 *Earthquake selection*

Accelerograms from seven well-known earthquakes recorded at stiff to intermediate soil sites were selected and DC filtered. Soft sites with distinct soil resonance effects were not chosen, neither were earthquakes with pulse type effects (near field). Large events were chosen so as to have a frequency content similar to the ultimate design event.

For comparative purposes two artificial ground motions were generated using SIMQKE to match the IBC spectra for site flexibilities B and D. These site categories bounded the site flexibilities of the calibration earthquakes.

7.3 *Damping correction factor*

A total of 14 damping correction factors for each of the 7 natural ground motions were used. The correction factors obtained are presented in Figure 7. Considerable scatter was noted, even

for a given earthquake. The "Lambda" values followed the erratic undulations of the ADRS plot for each event. From a bi-linear regression of the data, typically the EVD values based on the area method needed to be reduced by 28% across the post-yield range. The corrected damping curve is presented on Figure 5.

It was postulated that synthetic ground motions would give a smoother set of "Lambda" value data as large ADRS undulations would not be present. This was found to be the case, as can be observed in Figure 7.

7.4 *Comparison with other methods*

Prediction accuracy was checked using the ADRS for each of the 9 earthquakes and the displacement response results for each earthquake amplification.

Maximum displacement responses were predicted using the ATC-40 Type B hysteresis damping relationship. The actual response divided by the prediction is plotted in Figure 8 against overall global ductility. It can be seen that in the pre-yield ATC-40 over-predicts displacements due to the assumption of 5% damping. For moderate post-yield ductilities it typically under-predicts, with actual displacements exceeding predictions by up to 50%.

The FEMA 273 Co-efficient Method was also used. For the calibration structure the method condenses down to the equal displacement observation. The results are presented in Figure 9. As can be seen, the scatter is considerable with a tendency on average to under-predict displacements. In some instances actual displacements were found to be double the prediction.

Finally, using the bi-linear "Lambda" relationship determined above, and Freeman's Capacity Spectrum approach, displacement predictions were made. These are presented in Figure 10. It can be seen that the wider variation in the "Lambda" values translates into a smaller variation in displacement prediction. The prediction accuracy is more consistent across the full range of ductile response and typically the actual response rarely exceeded the prediction by more than 20%.

8 **DISCUSSION**

The provision of simple but accurate tools for displacement prediction is challenging. Fundamentally there is a problem in trying to represent a non-linear hysteretic system with a linear viscously damped system. For this reason a linear substitute structure can have only limited success. Additionally, with ground motion variability, prediction scatter is inherent.

The FEMA 273 Co-efficient Method, while giving a reasonable average prediction, has great scatter. Actual response may be double that predicted. The recommendation by Whittaker et al (Whittaker et al 1998) to increase predictions by 50% to upper-bound actual responses is supported by these limited findings.

The ATC-40 Type B hysteresis damping curves were a close match to the uncalibrated area method curves obtained for the single storey frame. The observed trends in prediction accuracy with global ductility demand could be reduced by optimising the damping values.

The work undertaken has in effect been an optimisation of the substitute structure method, and the results have been encouraging. Accuracy has been achieved for both serviceability and ultimate limit states. The predictable "Lambda" value trends for the synthetic ground motions have suggested that the capacity spectrum approach could be almost as accurate as Chopra's inelastic spectra approach for a given smoothed spectra.

The significant limitation in this work has been in the structure range and ground motions examined thus far. As most of the 9 ground motions used to assess accuracy were also used in calibration, optimistic findings could be anticipated. Nevertheless, unique damping curves could potentially be generated for a range of typical structural frame types and soil conditions

using the methodology presented, thereby permitting the designer to make more accurate displacement predictions.

9 CONCLUSION

The work presented demonstrates that a substitute structure methodology can be calibrated to provide an improved prediction of maximum displacement response when compared to other published methods.

10 ACKNOWLEDGEMENT

The work reported in this paper forms part of a project investigating the DBM funded by the Australian Research Council (Large Grant No. A89701689 and Small Grant No. 589711277)

REFERENCES:

Alsiwat J.M. and Saatcioglu M. 1992, Reinforcement anchorage slip under monotonic loading, *Journal of Structural Engineering, ASCE*. 118(9). 2421-2438.

Chopra A.K. and Rakesh K.G. 1999, Capacity–demand-diagram methods for estimating seismic deformation of inelastic structures : SDF systems, *PEERC*, Report No. PEER-1999/02.

Freeman S.A. 1998, The capacity spectrum method as a tool for seismic design, *Proc of 11th European Conference on Earthquake Engineering*.

Lam N.T.K. , Chandler A.M. , Wilson J.L. and Hutchinson, G.L. 2002, The prediction of displacement and velocity demand of long distance earthquakes, *Procs. of the 12th European Conf. on Eqke Eng*.

Pantazopoulou S. and Bonacci J. 1992, Consideration of questions about beam-column joints, *ACI Structural Journal*. 89(1). 27-36.

Park R and Paulay T. , 1975, Reinforced concrete structures", *Wiley*.

Priestley M.J.N. 1998, Brief comments on elastic flexibility of reinforced concrete frames and significance to seismic design, *Bulletin of the New Zealand Society for Earthquake Engineering*. 31(4). 246-259.

Priestley M.J.N. and Kowalsky M.J. 2000, Direct displacement-based seismic design of concrete buildings, *Bulletin of the New Zealand Society for Earthquake Engineering*. 33(4). 421-444.

Shibata A. and Sozen M.A. 1976, Substitute-structure method for seismic design in R/C, *Journal of Structural Engineering, ASCE*. 102(ST1). 1-18.

Soroushian P. and Choi K. 1991, Analytical Evaluation of Straight Bar Anchorage Design in Exterior Joints", *ACI Structural Journal*. 88(2). 161-168.

Whittaker A. , Constantinou M. and Tsopelas P. 1998, Displacement estimates for performance-based seismic design, *Journal of Structural Engineering, ASCE. 124(8). 905-912.*

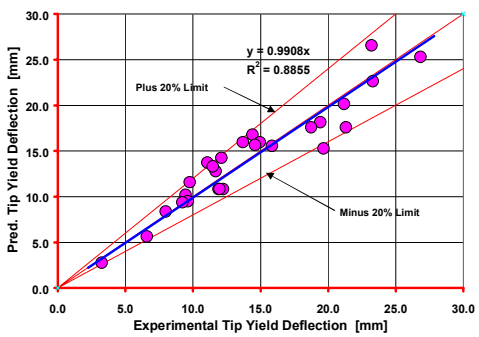

Figure 1 Beam Deflection Match at Yield

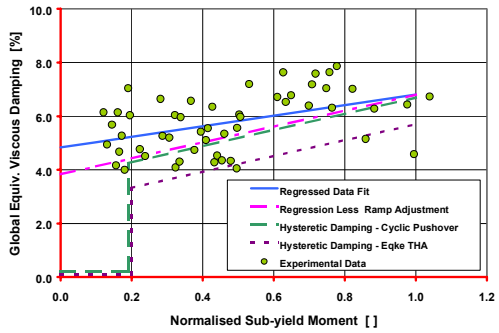

Figure 2 Hysteretic Sub-yield Damping

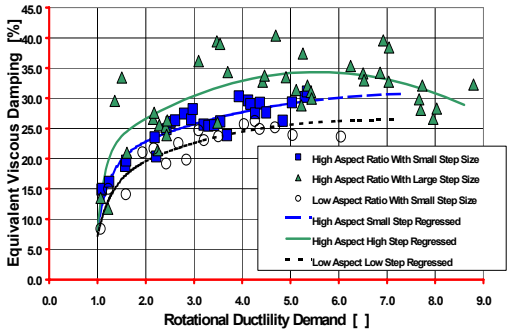

Figure 3 Beam Flexural Damping

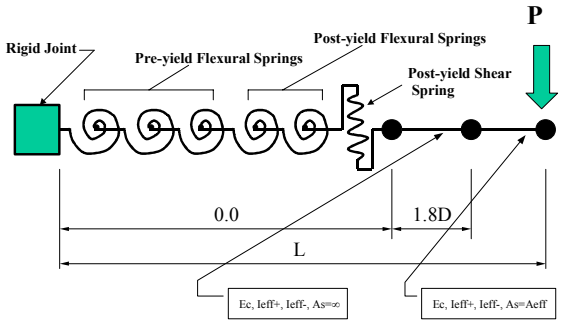

Figure 4 Beam Hinge Composite Springs

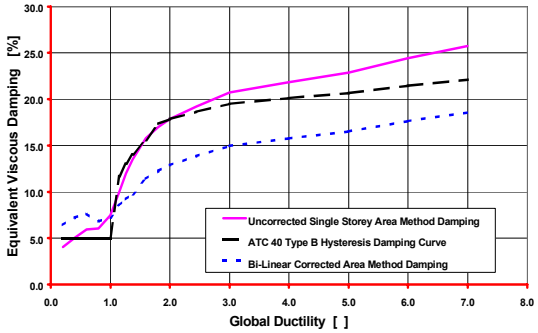

Figure 5 Single Storey Structure Global Damping Curves.

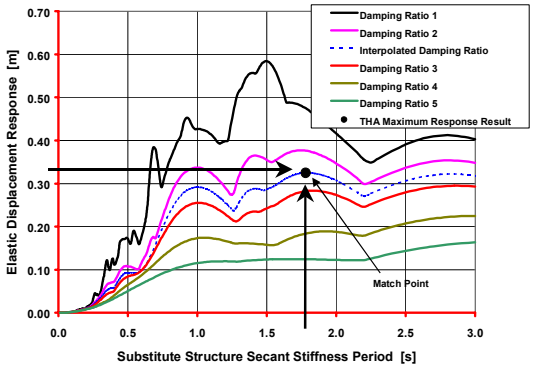

Figure 6 Calibration Method

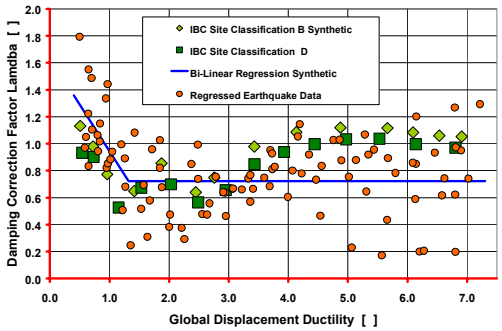

Figure 7 Correction Factor "Lambda" Data Regression

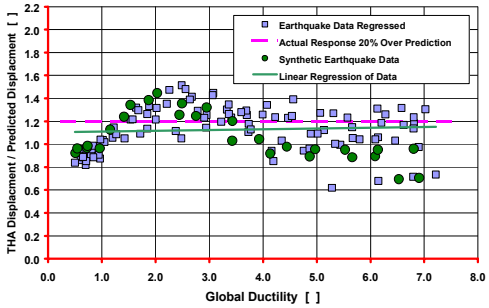

Figure 8 ATC-40 THA Prediction Results

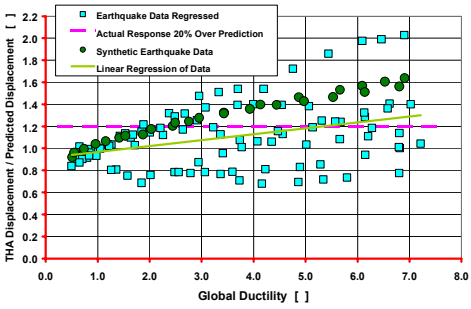

Figure 9 FEMA 273 Prediction Results

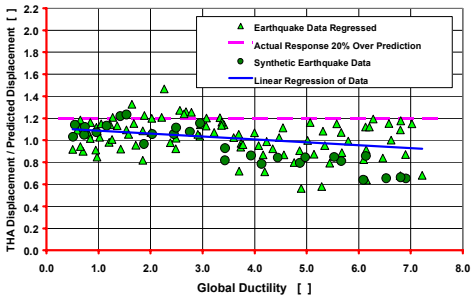

Figure 10 Calibrated Substitute Structure Prediction Accuracy